

CHAPTER V
SYNTHESIS, CHARACTERIZATION, AND CATALYTIC PERFORMANCE
OF Ti-MCM-48 FROM SILATRANE

5.1 Abstract

Titanium-containing MCM-48 was successfully synthesized via hydrothermal treatment using moisture-stable silatrane as a silica source. The materials were characterized by X-ray diffraction (XRD), N₂ adsorption-desorption measurement, Diffuse reflectance UV–vis spectroscopy (DR-UV), field emission scanning electron microscopy (FE-SEM), and transmission electron microscopy (TEM). Both XRD patterns and TEM images showed well-ordered 3D cubic pore structures of Ti-MCM-48. The materials possessed high specific surface area and reached 1,681 m²/g with 2.02 nm pore diameter and 0.85 cm³/g pore volume. SEM revealed the truncated-octahedral shape of the materials. The catalytic performance of Ti-MCM-48 materials on the oxidation of styrene oxidation using H₂O₂ as an oxidant resulted in the highest styrene conversion of 51.6%, giving styrene oxide and benzaldehyde at 40.1 and 59.9%, respectively, even at the lowest titanium loading onto MCM-48.

(Keywords: Silatrane, Ti-MCM-48, truncated-octahedral shape, oxidation of styrene)

5.2 Introduction

Due to environmental concerns and ease of separation, the heterogeneous catalysts have played important role in petrochemical area. Titanium(IV), one of the important transition-metal ions, has been introduced to the catalysts to enhance the catalytic properties. For several decades, Ti-incorporated microporous zeolites have been of interest due to their high catalytic properties in selective oxidation reactions [1]. However, with the small pores of zeolites limited the ability of bulk organic compounds to diffuse through them [2, 3]. To support the selective oxidation of the bulk organic molecules, Ti-containing mesoporous materials thus became a promising approach. Many efforts have been made toward the incorporation of Ti into the mesoporous silica by direct synthesis [2-9] or grafting method [10, 11]. MCM-48, another type of mesoporous silica, contains pore network, which possesses three-dimensional pores, allowing faster diffusion of reactants than the one-dimensional pores network of MCM-41 [3, 6]. Consequently, Ti-MCM-48 materials may have more advantages than other materials. However, Ti-MCM-48 has not been greatly studied probably owing to the difficulty of the preparation, as compared to other materials [1]. Besides, the applications of Ti-containing catalysts for the oxidation reactions — such as the epoxidation of methyl oleate [10], the epoxidation of cyclohexene [5], the oxidation of styrene [1,12] — have been widely reported.

Based on our previous works, we have successfully synthesized MCM-48 as well as chromium and cerium loading on MCM-48 using moisture-stable silatrane as silica source [13, 14]. In this article, we reported not only the synthesis of Ti-MCM-48 with different titanium loading via sol-gel process, but also its catalytic performance on the oxidation of styrene. The optimal conditions were also determined as functions of time, temperature, amount of catalyst, amount of oxidant, and amount of Ti loading.

5.3 Experimental

5.3.1 Materials

Ti-MCM-48 mesoporous materials were synthesized hydrothermally using fumed silica (SiO_2 , 99.8%, Sigma-Aldrich, USA), triethanolamine (TEA, Carlo Erba, Italy), ethylene glycol (EG, J.T. Baker, USA), acetonitrile (Labskan, Thailand), sodium hydroxide (NaOH, Labskan, Asia), cetyltrimethylammonium bromide (CTAB, Sigma-Aldrich, Denmark) and titanium(IV) butoxide (97%, Aldrich, USA). All chemicals were used without further purification.

5.3.2 Catalyst Preparation

To prepare Ti-MCM-48, CTAB, used as a structure-directing agent, was dissolved in a solution containing water and 2M NaOH. The mixture was stirred continuously with slight heating to dissolve CTAB, followed by adding a required amount of titanium butoxide. Then, our homemade silatrane was introduced into the mixture with continuous stirring for 1 h. The molar composition of the gel was $1.0 \text{ SiO}_2:0.3\text{CTAB}:0.50\text{NaOH}:62.0\text{H}_2\text{O}:x\text{Ti}$, where $0.01 \leq x \leq 0.1$. The resulting mixture was transferred to a Teflon-lined stainless steel autoclave and treated at 140 °C for 16 h. The resulting solid product was collected by filtration and dried overnight at ambient conditions. Removal of all organics was performed by calcinations at 550 °C for 6 h (Carbolite, CFS 1200, Hope Valley, U.K.) at a heating rate of 0.5 °C/min to obtain mesoporous Ti-MCM-48.

5.3.3 Catalyst Characterization

The structure pattern of the Ti-MCM-48 products was analyzed on an XRD (Rigaku, Japan) using $\text{CuK}\alpha$ radiation over the range of $2\theta = 2^\circ\text{-}60^\circ$ at a scanning speed of 1 °C/min, 40 kV, and 30 mA. The product morphology was examined using an FE-SEM (Hitachi/S-4800). The order of mesopores was investigated using a TEM (JEOL 2010F). The specific surface area and average pore size were estimated by the Brunauer-Emmett-Teller (BET) method on a Quantasorb JR instrument (Mount Holly, NJ). DR-UV-Vis spectra of samples were recorded

from 200 to 600 nm on a Shimadzu UV-2550 spectrophotometer using BaSO₄ as a reference.

5.3.4 Activity Study of Ti-MCM-48

The oxidation of styrene was proposed to study the catalytic activity of Ti-MCM-48 samples. The reaction mixture containing styrene (5 mmol), a desired amount of 30% H₂O₂, acetonitrile (5ml), and Ti-MCM-48 (0.025-0.1g) was stirred in a glass flask. The reaction time and temperature were varied in the range of 2-6h and 60-80°C, respectively. The products were analyzed on a gas chromatograph (GC) equipped with a capillary column (ZB-Wax, 0.25mm I.D., 30m) and FID detector. The conversion of styrene was calculated based on the amount of styrene monomer consumed using an internal standard method. Each analysis was made in triplicate.

5.4 Results and Discussion

5.4.1 Catalyst Characterization

The low-angle XRD patterns of the calcined Ti-MCM-48 with different Ti loadings are shown in Fig. 5.1(a). It can be seen that Ti-MCM-48 samples with the mole of Ti loading in the range of 0.01-0.05 preserved the MCM-48 parent materials and showed a well-resolved XRD pattern of cubic *Ia3d* space group [15, 16]. As the Ti content was increased up to 0.1 Ti/Si ratio, the MCM-48 structure collapsed, as can be seen from the poor XRD pattern. These results were consistent with the studies cited elsewhere [2, 9] which also synthesized Ti-MCM-41 with various contents of Ti. They found that the crystallinity of Ti-MCM-41 samples was lost and the intensity of d₂₁₁ peak was lower as the titanium contents increased. Moreover, they also obtained a lower intensity of [100] reflection peak at high percentages of Ti-MCM-41, indicating the less-crystalline of the samples.

At wide angle range of the diffractograms in Fig. 5.1(b), there were no reflections of Ti anatase phase, implying the absence of the bulk anatase and high dispersion of titanium oxide in the framework. This result was in agreement with the

study of Zhao *et al.* [17]. Otherwise, it can be pointed out that the TiO₂ crystals are very tiny and lower than the XRD detection limit [18].

Textural properties of calcined Ti-MCM-48 are summarized in Table 5.1. The incorporation of Ti caused a decrease in BET specific surface area as well as the pore volume, consistent with the results obtained by Nath and Ganguli [3]. Figure 5.2 shows the nitrogen adsorption-desorption isotherms of all samples. All patterns can be classified into the type IV isotherm, indicating mesoporous materials. Moreover, the sharp inflections at relative pressures (P/P_0) between 0.2 and 0.4 of the Ti-MCM-48 samples with the Ti/Si ratios between 0.01 and 0.05 indicated a uniform pore size distribution (see the BJH pore size distributions in Fig. 5.3). Unlike the sample prepared at the 0.07 ratio, it appeared to be less order of the materials which can be supported by the XRD results in Fig. 5.1.

DR-UV-Vis spectra of the calcined Ti-MCM-48 samples are given in Fig. 5.4. The absorption band at 210-220 nm was assigned to Ti⁴⁺ ions in the tetrahedral coordinate site [18]. The absorption shoulder band at 260-270 nm was probably due to the occurrence of the site-isolated Ti atoms in penta- or octahedral coordination [2]. The bulk titania usually appears as a broad absorption band at 330 nm which was found in the Ti-MCM-48 samples with ratios above 0.05. The overall results may imply that most of the Ti atoms occupied a site isolated in silica framework which was found in the Ti-MCM-48 samples with 0.01 and 0.03 ratios.

The morphology and pore structure of the synthesized Ti-MCM-48 were observed by both FE-SEM and TEM techniques, as shown in Fig. 5.5 and 5.6. Analysis revealed that the calcined Ti-MCM-48 materials with Ti/Si ratios of 0.01-0.07 formed a truncated-octahedral shape which preserved the MCM-48 parent material shape [13]. The size of particles decreased as increasing Ti/Si ratios due to the presence of many nuclei of metal ion content in the solution. Furthermore, the TEM images with the incident along directions [100] and [110], which was a characteristic of MCM-48, were also found in the samples (Fig. 5.6). It could be confirmed that the highly ordered cubic pore structure of Ti-MCM-48 was obtained and consistent with the XRD results.

5.4.2 Activity Study of Ti-MCM-48

The catalytic properties of all synthesized Ti-MCM-48 samples were studied on the styrene epoxidation reaction. The main products obtained from this reaction were benzaldehyde and styrene oxide. To achieve the highest styrene conversion, various parameters, viz. reaction time, reaction temperature, amount of oxidant, amount of catalyst and amount of Ti content, were examined. The catalytic results are summarized in Table 5.2. Considering the effect of the reaction time at 80°C using 0.05 g of Ti-MCM-48 with 0.01 Ti/Si (see entries 3, 4, and 5), the conversion of styrene monomer reached the highest yield (51.6%) at 6 h reaction time while the selectivity of styrene oxide slightly decreased as the reaction time increased. These results were consistent with the investigation by Samran *et al.* [20]. Thus, the 6 h reaction time was selected for further study.

As the reaction temperature was increased (entries 5, 6 and 7) and other parameters remained constant, the conversion of styrene increased, a result agreeing well with reports described elsewhere [8, 21]. It should be noted that not only the conversion of styrene did favor a high temperature, but also that the selectivity of the styrene oxide increased, albeit slightly. These results were in harmony with the study of Adam and Iqbal [22].

Interestingly, the amount of the oxidant, H₂O₂, affected the styrene conversion as well as the benzaldehyde selectivity. It was found that as the mole ratio of H₂O₂:styrene was increased to 2:1 (as shown in entries 5, 8, and 9), the styrene conversion and the benzaldehyde selectivity were enhanced to 59 and 93%, respectively. These results were consistent with works described by Wang *et al.* [23] and Liu *et al.* [24]. This might be attributed to the further oxidation process of styrene oxide and the oxidative cleavage of C=C bond resulting in benzaldehyde which was promoted by the excess of H₂O₂ [24].

The effect of the catalyst amount can be found in the entries 5, 10, and 11. As expected, the conversion of the styrene increased from 39 to 62% while the quantity of the catalyst was increased. However, the selectivity toward styrene oxide decreased when using catalyst as high as 0.1 g. Again, this might have resulted from the further oxidation of the styrene oxide product [20, 25].

Compared to the pure MCM-48 (entry 2), all Ti-MCM-48 (entries 5, 12, 13 and 14) provided higher styrene conversion (from 2.8 to 51.6%). This could

indicate that the higher styrene conversion was due to the presence of active Ti centers. However, the styrene conversion did not improve while Ti/Si ratios above 0.03 were increased. This probably resulted from the presence of Ti extraframework, as confirmed by DR-UV spectrum (Fig. 5.4), which was not active for the reaction.

Considering the activity of other catalysts toward styrene oxidation, e.g. Samran *et al* [20] and Cojocariu *et al* [21] studied Ti-SBA-15 and TiO₂-SiO₂ xerogel, respectively, as compared to Ti-MCM-48 in this work, it was found that the Ti-MCM-48 provided higher not only %conversion but also %selectivity of styrene oxide. It might be that Ti-MCM-48 possessed high specific area, providing more Ti active sites than others. However, in this study, the %selectivity of styrene oxide was lower than benzaldehyde in all cases. Cojocariu *et al.* [21] suggested that the addition step of H₂O₂ to the reaction solution affected the products distribution. Adding H₂O₂ dropwise over 120 min resulted in much higher %selectivity of styrene oxide. Thus, the higher %selectivity of styrene oxide could be obtained if the H₂O₂ was added dropwise into the solution.

5.5 Conclusions

Highly ordered mesoporous Ti-MCM-48 was successfully synthesized via hydrothermal process. The synthesized products provided high specific surface area and narrow pore size distribution. SEM images exhibited the truncated-octahedral shape of Ti-MCM-48 samples although the extraframework of bulk TiO₂ was observed at high Ti loadings, as confirmed by DR-UV. The catalytic performances of Ti-MCM-48 samples on styrene epoxidation reaction showed that Ti-MCM-48 with 0.01 Ti/Si ratio was the most effective catalyst and provided the maximum conversion of styrene (51.6%) at 80°C for 6h. The selectivity of styrene oxide and benzaldehyde reached 40.1% and 59.9%, respectively.

5.6 Acknowledgements

This research is financially supported by the Thailand Research Fund and the Center for Petroleum, Petrochemicals, and Advanced Materials, Chulalongkorn

University, Thailand. The authors would like to thank Mr. John M. Jackson for English proofreading.

5.7 References

- [1] Ji, D., Zhao, R., Lv, G., Qian, G., Yan, L., and Suo, J. (2005) Direct synthesis, characterization and catalytic performance of novel Ti-SBA-1 cubic mesoporous molecular sieves. *Appl. Catal., A*, 281(1–2), 39-45.
- [2] Yu, J., Feng, Z., Xu, L., Li, M., Xin, Q., Liu, Z., and Li, C. (2001) Ti-MCM-41 Synthesized from Colloidal Silica and Titanium Trichloride: Synthesis, Characterization, and Catalysis. *Chem. Mater.*, 13(3), 994-998.
- [3] Nath, B. and Ganguli, J.N. (2011) Synthesis, Characterization and Catalytic Application of Ti-MCM-48. *BCSI*, 9, 9-15.
- [4] Øye, G., Sjöblom, J., and Stöcker, M. (2000) Synthesis and Characterization of the Titanium Containing Mesoporous Molecular Sieve MCM-48. *J. Dispersion Sci. Technol.*, 21(1), 49-63.
- [5] Peña, M. L., Dellarocca, V., Rey, F., Corma, A., Coluccia, S. and Marchese, L. (2001) Elucidating the local environment of Ti(IV) active sites in Ti-MCM-48: a comparison between silylated and calcined catalysts. *Micropor. Mesopor. Mater.*, 44–45(0), 345-356.
- [6] Yuan, S., Shi, L., Mori, K., and Yamashita, H. (2008) Synthesis of Ti-containing MCM-48 by using TiF₄ as titanium source. *Mater. Lett.*, 62(17–18), 3028-3030.
- [7] Gontier, S. and Tuel, A. (1995) Synthesis and characterization of Ti-containing mesoporous silicas. *Zeolites*, 15(7), 601-610.
- [8] Hulea, V. and Dumitriu, E. (2004) Styrene oxidation with H₂O₂ over Ti-containing molecular sieves with MFI, BEA and MCM-41 topologies. *Appl. Catal., A*, 277(1–2), 99-106.
- [9] Thanabodeekij, N., Tanglumlert, W., Gulari, E., and Wongkasemjit, S. (2005) Synthesis of Ti-MCM-41 directly from silatrane and titanium glycolate and its catalytic activity. *Appl. Organomet. Chem.*, 19(9), 1047-1054.

- [10] Guidotti, M., Gavrilova, E., Galarneau, A., Coq, B., Psaro, R., and Ravasio, N. (2011) Epoxidation of methyl oleate with hydrogen peroxide. The use of Ti-containing silica solids as efficient heterogeneous catalysts. Green Chem., 13(7), 1806-1811.
- [11] Calleja, G., van Grieken, R., Garcia, R., Melero, J. A., and Iglesias, J. (2002) Preparation of titanium molecular species supported on mesostructured silica by different grafting methods. J. Mol. Catal. A: Chem., 182–183(0), 215-225.
- [12] Chen, Y., Huang, Y., Xiu, J., Han, X., and Bao, X. (2004) Direct synthesis, characterization and catalytic activity of titanium-substituted SBA-15 mesoporous molecular sieves. Appl. Catal., A, 273(1–2), 185-191.
- [13] Longloilert, R., Chaisuwan, T., Luengnaruemitchai, A., and Wongkasemjit, S. (2011) Synthesis of MCM-48 from silatrane via sol–gel process. J. Sol-Gel Sci. Technol., 58(2), 427-435.
- [14] Longloilert, R., Chaisuwan, T., Luengnaruemitchai, A., and Wongkasemjit, S. (2012) Synthesis and characterization of M-MCM-48 (M = Cr, Ce) from silatrane via sol–gel process. J. Sol-Gel Sci. Technol., 61(1), 133-143.
- [15] Schmidt, R., Stocker, M., Akporiaye, D., Torstad, E. H., and Olsen, A. (1995) High-resolution electron microscopy and X-ray diffraction studies of MCM-48. Microporous Mater., 5(1), 1-7.
- [16] Alfredsson, V. and Anderson, M. W. (1996) Structure of MCM-48 Revealed by Transmission Electron Microscopy. Chem. Mater., 8(5), 1141-1146.
- [17] Zhao, D., Budhi, S., Rodriguez, A., and Koodali, R. T. (2010) Rapid and facile synthesis of Ti-MCM-48 mesoporous material and the photocatalytic performance for hydrogen evolution. Int. J. Hydrogen Energy, 35(11), 5276-5283.
- [18] Schrijnemakers, K. and Vansant, E. F. (2001) Preparation of Titanium Oxide supported MCM-48 by the designed dispersion of Titanylacetylacetonate. J. Porous Mater., 8(2), 83-90.
- [19] Luo, Y., Lu, G. Z., Guo, Y. L., and Wang, Y. S. (2002) Study on Ti-MCM-41 zeolites prepared with inorganic Ti sources: Synthesis, characterization and catalysis. Catal. Comm., 3(3), 129-134.

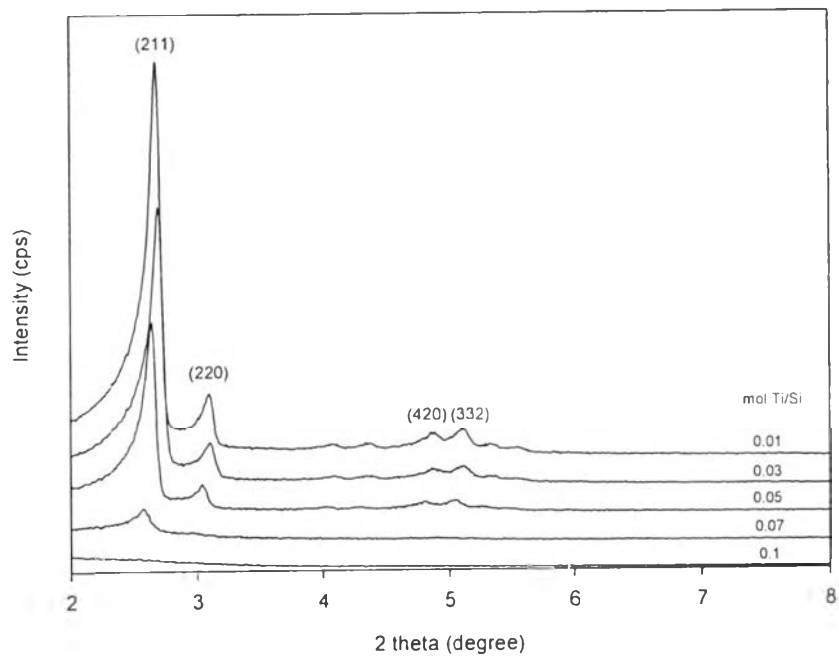
- [20] Samran, B., Aungkutrannont, S., White, T., and Wongkasemjit, S. (2011) Room temperature synthesis of Ti-SBA-15 from silatrane and titanium-glycolate and its catalytic performance towards styrene epoxidation. J. Sol-Gel Sci. Technol., 57(2), 221-228.
- [21] Cojocariu, A. M., Mutin, P. H., Dumitriu, E., Fajula, F., Vioux, A., and Hulea, V. (2010) Mild oxidation of bulky organic compounds with hydrogen peroxide over mesoporous TiO₂-SiO₂ xerogels prepared by non-hydrolytic sol-gel. Appl. Catal., B, 97(3-4), 407-413.
- [22] Adam, F. and Iqbal, A. (2010) The oxidation of styrene by chromium-silica heterogeneous catalyst prepared from rice husk. Chem. Eng. J., 160(2), 742-750.
- [23] Wang, Y., Zhang, Q., Shishido, T., and Takehira, K. (2002) Characterizations of Iron-Containing MCM-41 and its catalytic properties in Epoxidation of Styrene with Hydrogen Peroxide. J. Catal., 209(1), 186-196.
- [24] Zhang, W.-H., Lu, J., Han, B., Li, M., Xiu, J., Ying, P., and Li, C. (2002) Direct synthesis and characterization of Titanium-Substituted Mesoporous Molecular Sieve SBA-15. Chem. Mater., 14(8), 3413-3421.
- [25] Laha, S. C. and Kumar, R. (2001) Selective epoxidation of styrene to styrene oxide over TS-1 using Urea-Hydrogen peroxide as oxidizing agent. J. Catal., 204(1), 64-70.

Table 5.1 The characteristics of the calcined samples with a molar gel composition of $1.0\text{SiO}_2:0.3\text{CTAB}:0.50\text{NaOH}:62.0\text{H}_2\text{O}:x\text{Ti}$ where $0.01 \leq x \leq 0.07$

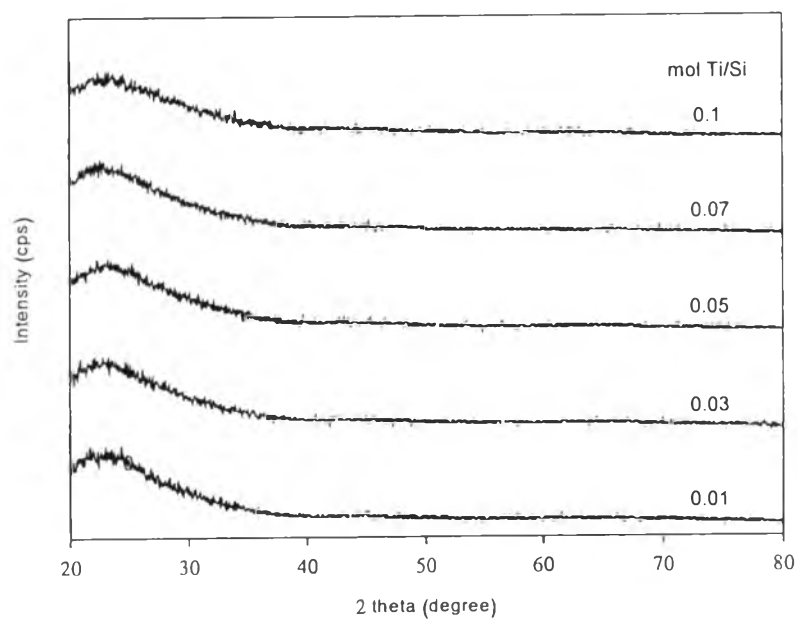
Sample	S_{BET} (m^2/g)	Pore volume (cm^3/g)	Pore diameter (nm)	a_0 (nm)	Wall thickness (nm)
MCM-48	1,711	1.14	2.67	8.66	1.47
Ti-MCM-48-(0.01)	1,681	0.85	2.02	8.11	1.61
Ti-MCM-48-(0.03)	1,377	0.72	2.10	8.05	1.55
Ti-MCM-48-(0.05)	1,124	0.63	2.26	8.20	1.52
Ti-MCM-48-(0.07)	555	0.33	2.36	8.42	1.55

Table 5.2 Catalytic performances for the oxidation of styrene using MCM-48 and Ti-MCM-48-x (x = Ti/Si ratio)

Entry	Catalyst	Time (h)	Temperature (°C)	Mole ratio H ₂ O ₂ :styrene	Amount of catalyst (g)	% Conversion	% Selectivity	
							Benzaldehyde	Styrene oxide
1	blank	6	80	1:1	-	3.1±0.34	18.3±1.68	81.7±1.68
2	MCM-48	6	80	1:1	0.05	2.8±0.33	43.0±2.86	57.0±2.86
3	Ti-MCM-48-0.01	2	80	1:1	0.05	32.2±1.58	52.2±1.18	47.8±1.18
4	Ti-MCM-48-0.01	4	80	1:1	0.05	35.1±2.53	57.4±0.79	42.6±0.79
5	Ti-MCM-48-0.01	6	80	1:1	0.05	51.6±0.92	59.9±1.83	40.1±1.83
6	Ti-MCM-48-0.01	6	70	1:1	0.05	43.0±1.29	60.4±3.56	39.6±3.56
7	Ti-MCM-48-0.01	6	60	1:1	0.05	29.5±1.08	65.7±2.81	34.3±2.81
8	Ti-MCM-48-0.01	6	80	0.5:1	0.05	37.8±2.03	44.8±2.17	55.2±2.17
9	Ti-MCM-48-0.01	6	80	2:1	0.05	58.8±0.29	92.7±1.65	7.3±1.65
10	Ti-MCM-48-0.01	6	80	1:1	0.025	39.0±1.70	54.9±0.77	45.1±0.77
11	Ti-MCM-48-0.01	6	80	1:1	0.1	61.9±2.06	72.8±2.51	27.2±2.51
12	Ti-MCM-48-0.03	6	80	1:1	0.05	50.4±1.77	72.2±1.16	27.8±1.16
13	Ti-MCM-48-0.05	6	80	1:1	0.05	27.5±1.93	67.2±3.30	32.8±3.30
14	Ti-MCM-48-0.07	6	80	1:1	0.05	9.9±2.43	68.3±2.92	31.7±2.92



(a)



(b)

Figure 5.1 XRD patterns of the calcined Ti-MCM-48 samples with different Ti contents, taken at (a) low-angle and (b) wide-angle.

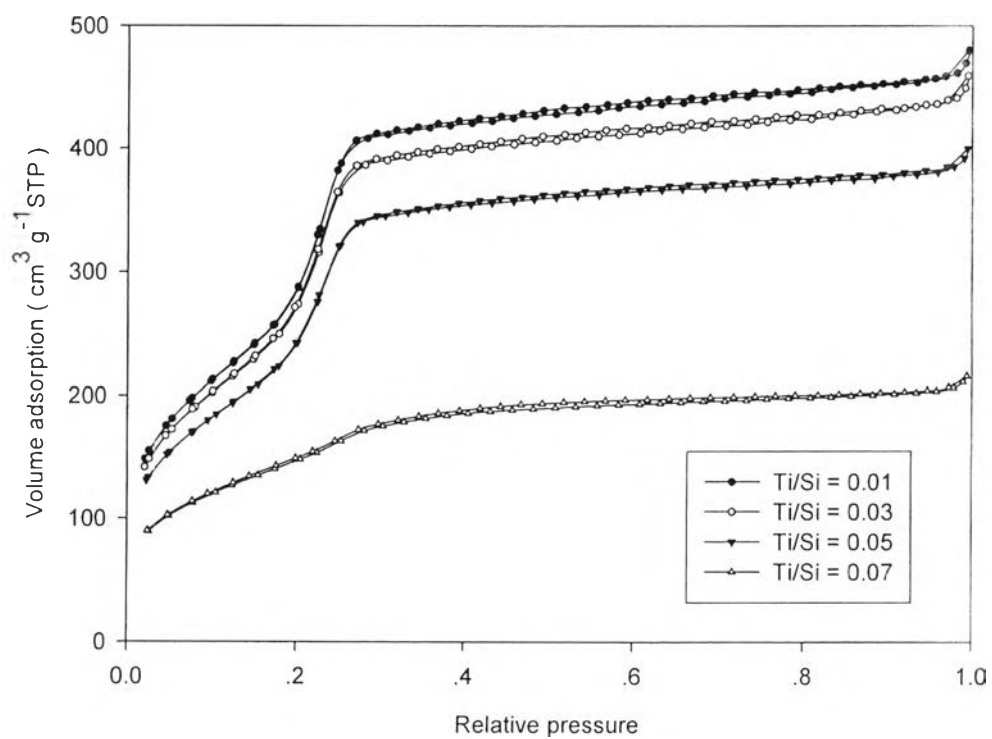


Figure 5.2 The N₂ adsorption and desorption isotherms of calcined Ti-MCM-48 with different Ti/Si ratios.

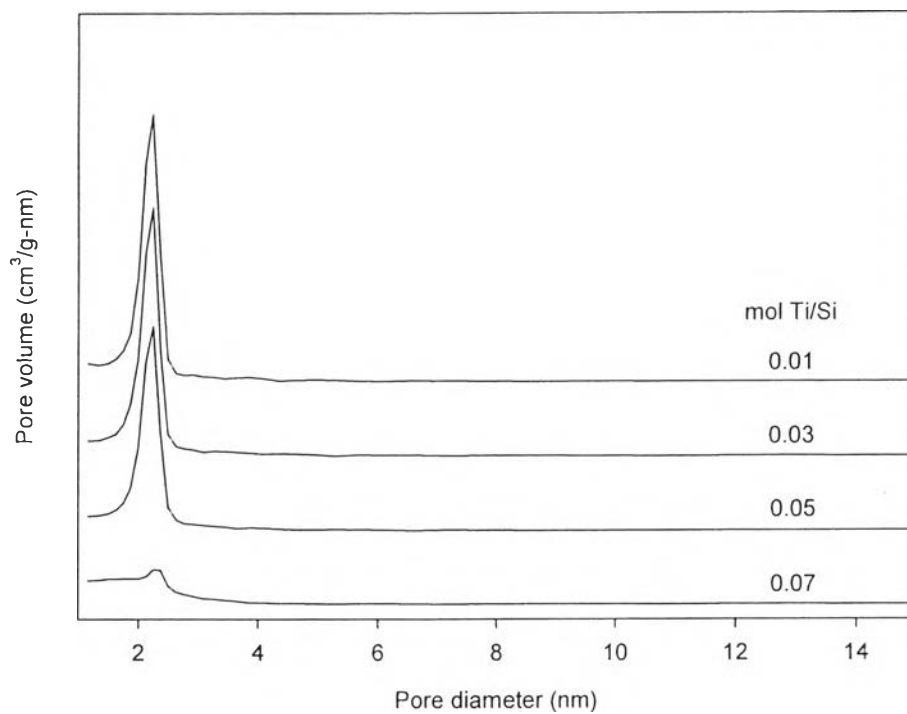


Figure 5.3 The BJH pore-size distributions (calculated from desorption branch of isotherm) of the calcined Ti-MCM-48 with different Ti/Si ratios.

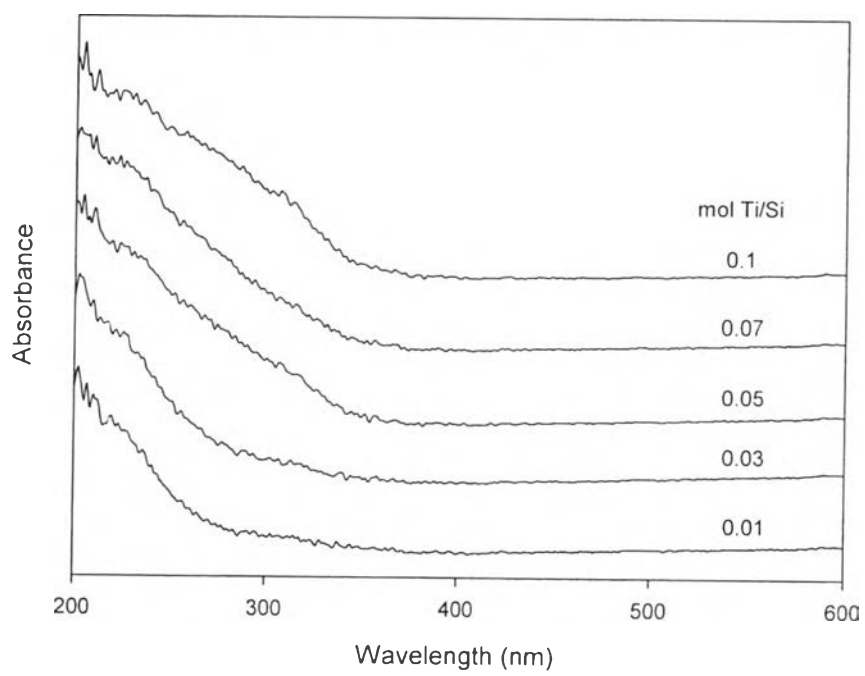
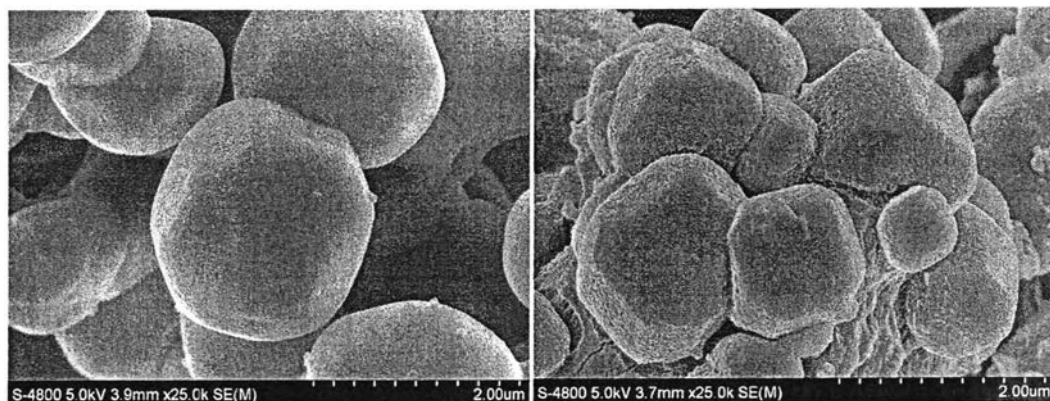
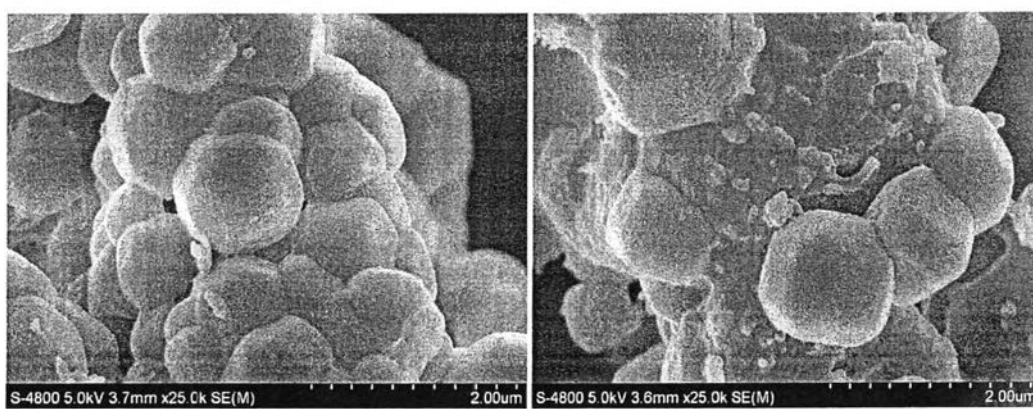


Figure 5.4 DR-UV-Vis spectra of the calcined Ti-MCM-48 with different Ti/Si ratios.



(a)

(b)



(c)

(d)

Figure 5.5 SEM images (x25000) of the calcined Ti-MCM-48 with different Ti/Si ratios (a) 0.01, (b) 0.03, (c) 0.05 and (d) 0.07.

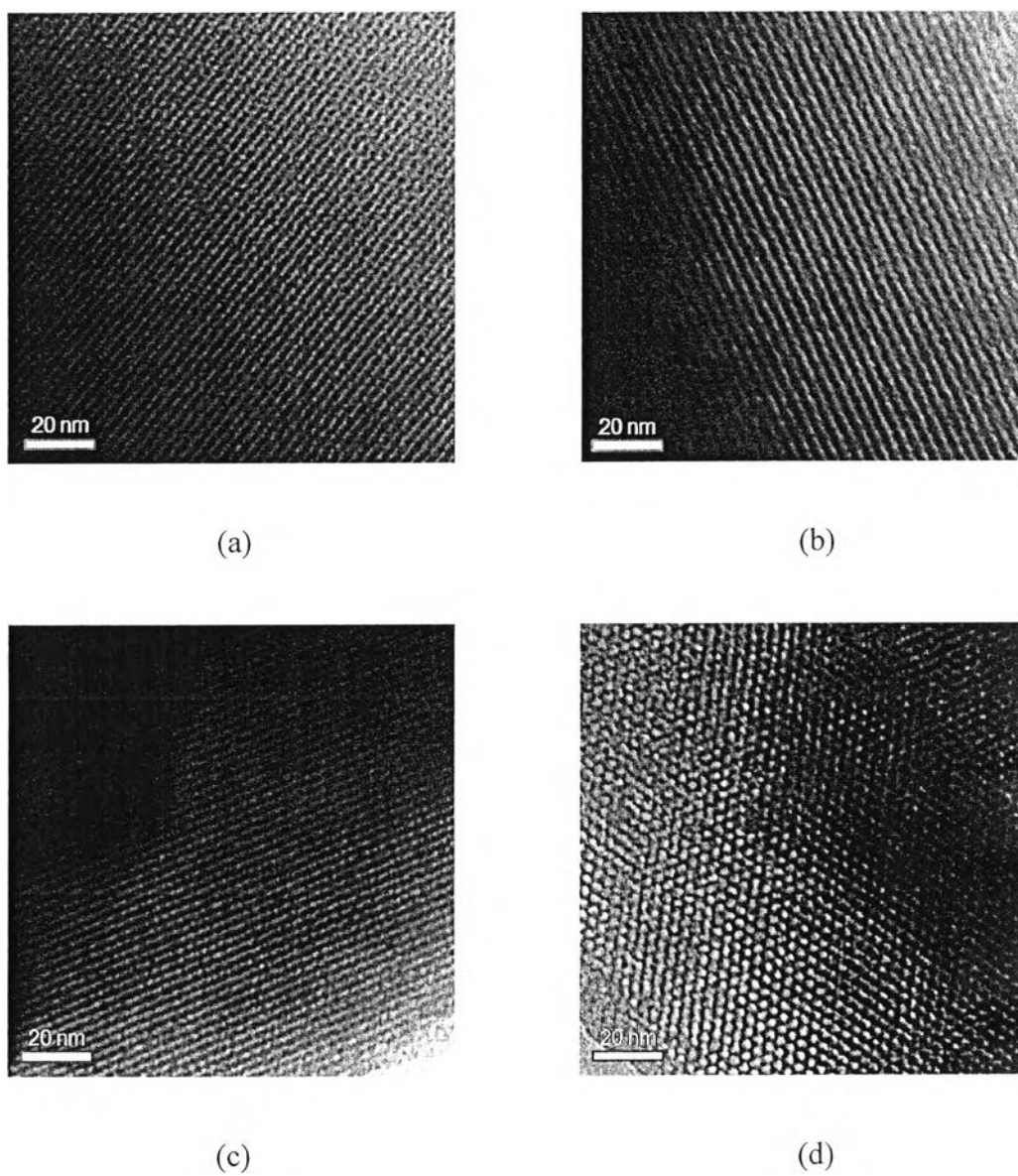


Figure 5.6 TEM images of the calcined Ti-MCM-48 with different Ti/Si ratios and incident along directions [100] of (a) 0.01, (b) 0.03, (c) 0.05, and [110] of (d) 0.07.